

Adversarial Hubness in Multi-Modal Retrieval

Tingwei Zhang
Cornell Tech
New York, USA
tingwei@cs.cornell.edu

Fnu Suya
University of Tennessee
Knoxville, USA
suya@utk.edu

Rishi Jha
Cornell Tech
New York, USA
rjha@cs.cornell.edu

Collin Zhang
Cornell Tech
New York, USA
collinzhang@cs.cornell.edu

Vitaly Shmatikov
Cornell Tech
New York, USA
shmat@cs.cornell.edu

Abstract

Hubness is a phenomenon in high-dimensional vector spaces where a single point from the natural distribution is unusually close to many other points. This is a well-known problem in information retrieval that causes some items to accidentally (and incorrectly) appear relevant to many queries.

In this paper, we investigate how attackers can exploit hubness to turn *any* image or audio input in a multi-modal retrieval system into an *adversarial* hub. Adversarial hubs can be used to inject universal adversarial content (e.g., spam) that will be retrieved in response to thousands of different queries, as well as for targeted attacks on queries related to specific, attacker-chosen concepts.

We present a method for creating adversarial hubs and evaluate the resulting hubs on benchmark multi-modal retrieval datasets and an image-to-image retrieval system implemented by Pinecone, a popular vector database. For example, in text-caption-to-image retrieval, a single adversarial hub, generated with respect to 100 randomly selected target queries, is retrieved as the top-1 most relevant image for more than 21,000 out of 25,000 test queries (by contrast, the most common natural hub is the top-1 response to only 102 queries), demonstrating the strong generalization capabilities of adversarial hubs. We also investigate whether techniques for mitigating natural hubness are an effective defense against adversarial hubs, and show that they are not effective against hubs that target queries related to specific concepts.

1 Introduction

Cross-modal and multi-modal retrieval systems that enable flexible and accurate information retrieval across different modalities (e.g., text-to-image, image-to-image, and text-to-audio) have drawn significant attention in recent years [72–74]. Modern retrieval systems leverage pretrained multi-modal encoders, such as ImageBind [22] and AudioCLIP [26], which encode inputs from different modalities (e.g., images and texts) into the same embedding space. In this shared space, semantically related inputs are clustered together (see Section 2), allowing queries encoded in the same space to be effectively matched based on similarity measures [56]. As a result, embedding-based retrieval is more scalable and accurate than traditional techniques based on metadata or keywords [3, 33].

These high-dimensional embedding spaces are prone to *hubness*—well-known problem in the information retrieval literature [44, 54] and one manifestation of the curse of dimensionality [54]. Hubness is a phenomenon where a point (a “natural hub”) appears in the neighborhood of many other points to which it is not semantically

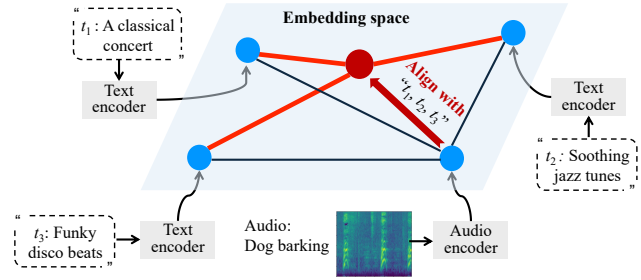


Figure 1: Cross-modal adversarial hub.

related. Many methods have been proposed for mitigating natural hubness [29, 32, 57, 57, 68, 82], including methods specifically for multi-modal retrieval [4, 13, 75] since it is especially vulnerable to hubness [40].

In this paper, we investigate whether hubness can be exploited to intentionally create images and audio inputs that act as “adversarial hubs.” Adversarial hubs (1) carry adversarial content, e.g., spam or misinformation, and (2) are very close in the embedding space to many queries in the same or different modality, causing them to be retrieved in response to these queries. For example, Figure 1 shows that a mild perturbation can align an audio clip of a barking dog to many unrelated text captions, including “A classical concert”, “Soothing jazz tunes”, and “Funky disco beats”, causing it to be retrieved whenever users search for any of these music genres. Figures 2, 3 and 4 illustrate concrete examples of adversarial hubs for different cross-modal retrieval scenarios.

Prior research on vulnerabilities in embedding-based retrieval focused on targeted adversarial alignment [85], poisoning of text-only retrieval corpora [10, 88], and uni-modal adversarial hubs in music recommendation [29]. Many works also focus on multi-modal adversarial examples whose objectives are related to downstream models rather than embeddings, such as jailbreaking LLM generation and causing misclassification of multi-modal inputs (see Section 8). Adversarial hubs are the first cross-modal attack on retrieval systems that affect multiple queries simultaneously—whether it be all queries or only those related to a specific concept.

Our Contributions. First, we show that hubness—a natural phenomenon in high-dimensional spaces where only a few data points become hubs—can be adversarially exploited. By applying a small perturbation generated with standard techniques, attackers can transform any image or audio input with chosen semantics (e.g., an

Query	Result
Golf cart perfect for courses	
Cooler looking sports car	
Small car that is easy to park in the city	

Figure 2: An adversarial hub in text-to-image retrieval.

Query	Result

Figure 3: An adversarial hub in image-to-image retrieval.

advertisement, product promotion, or song) into an adversarial hub that is retrieved in response to many queries in an embedding-based cross-modal retrieval system.

Second, we show that a single adversarial hub affects significantly more semantically unrelated queries than natural hubs. These attacks can also target specific concepts, so that the hub is retrieved only in response to queries related to that concept but not others. We evaluate hubness attacks on the same benchmarks as prior work [4, 13, 75], and also on a realistic image-to-image retrieval system developed by Pinecone [51]. We further evaluate existing techniques for mitigating natural hubness and show that they fail to mitigate concept-specific adversarial hubs even if hub generation is oblivious of the defense.

Third, we investigate transferability of adversarial hubs across different embeddings, and feasibility of generating them without knowledge of the target embedding model and query distribution.

Our results highlight a new risk to embedding-based, multi-modal retrieval systems, and we hope that they will motivate research on adversarially robust multi-modal embeddings. To facilitate research on the security of multi-modal embeddings, we released our code and models.¹

Query	Result
Christmas music	
Rock music	
Classical music	

Figure 4: An adversarial hub in text-to-audio retrieval.

2 Multi-Modal Retrieval

Traditional retrieval systems relied on hand-crafted features and metadata. Features such as SIFT and color histograms for images [45] and TF-IDF for text [55] provided basic representations that captured low-level information. Metadata, such as tags, labels, or captions, helped bridge different modalities by aligning co-occurring information, as in early image annotation systems [3, 33].

With the rise of deep learning, the field shifted toward models such as CLIP [53], pretrained on massive datasets to produce embeddings, which are dense vector representations of inputs. Embeddings map semantically related inputs from the same or different modalities (e.g., images and texts) into a shared latent space, greatly improving accuracy for both single-modal and cross-modal retrieval tasks. Typically, encoders into the embedding space are trained to minimize cosine similarity between related inputs, which helps ensure that their embeddings are neighbors [58].

Multi-Modal Embeddings. A multi-modal encoder θ^m transforms inputs from some modality $m \in \mathcal{M}$ into a common embedding space. We focus on systems with two modalities, but extending to more modalities is straightforward: generate bi-modal input pairs for different modality combinations and train as below.

Given a bi-modal dataset $D = (X, Y) \in m_1 \times m_2$, where (x, y) are semantically aligned (for instance, an image of a car and the text caption “Cars”), contrastive learning [48] is used to train the encoders by bringing embeddings of aligned pairs closer while pushing embeddings of unaligned inputs apart.

¹https://github.com/Tingwei-Zhang/adv_hub

Cross-Modal Retrieval. Consider an image retrieval system, consisting of (1) a vector database with embeddings of images, aka “Gallery”, and (2) “Queries” submitted by users in order to retrieve relevant images from the gallery. Queries can be in the same or different modality as the gallery. In text-to-image retrieval, queries are text captions (e.g., descriptions of cats), whereas in image-to-image retrieval queries are images (e.g., cat pictures). We use m_1 to denote the modality of queries and m_2 to denote the modality of the gallery data. Let $Q = \{q_i\}_{i=1}^N$ denote the queries and $G = \{g_i\}_{i=1}^S$ the vectors corresponding to the gallery. Let $\theta^{m_1}(\cdot)$ be the encoder for queries, $\theta^{m_2}(\cdot)$ for the gallery.

The retrieval system encodes the query and measures the cosine similarity of the resulting embedding with each data point in the gallery $g_j \in G$ as $\text{sim}(q_i, g_j) = \cos(\theta^{m_1}(q_i), \theta^{m_2}(g_j))$, then ranks all gallery data points from high to low based on their similarity to q_i , $\text{sort}(\text{sim}(q_i, g_1), \dots, \text{sim}(q_i, g_S))$, and finally returns the top k most relevant gallery data points.

3 Threat Model and Attack Methods

We describe the attacker’s goals in Section 3.1, then their knowledge and capabilities in Section 3.2, and then present the adversarial hubness attack in Section 3.3.

3.1 Attacker’s Goals

Figure 5 shows an overview of the threat model. The attacker aims to inject a maliciously crafted input g_a into the gallery that will act as an “adversarial hub.” The goal of the attack is to ensure that the hub’s embedding appears among the most relevant results (i.e., closest in the embedding space) to any query submitted by the user, in the same or different modality. The adversarial hub should achieve high relevance scores for many unrelated queries, even though the content of g_a is semantically irrelevant to these queries.

Types of Adversarial Hubs. We distinguish between two types of hubs. *Rational* hubs possess human-understandable semantics and can be driven by economic or other incentives—such as promoting products or songs, or spreading misinformation—whereas *reckless* hubs lack semantic meaning and are designed solely to disrupt retrieval performance through a denial-of-service. We focus primarily on rational hubs, since they are associated with practical threats to real-world retrieval systems, but our techniques for generating adversarial hubs work the same for either hub type.

Injecting adversarial hubs is straightforward when galleries contain user-generated data. For example, an attacker can post a hub online and wait for it to be indexed or added by users into their galleries [6]. In e-commerce applications, the attacker can include the hub in product descriptions. We focus on attacks involving a single hub, but an attacker can also control multiple inputs [91].

We consider two adversarial objectives: (1) *indiscriminate* attacks that aim to impact all queries, and (2) *concept-specific* attacks that aim to impact only certain queries in the interest of attackers. Both types of hubs can be used for both objectives.

Indiscriminate Objective. This attack aims to ensure that the adversarial hub is close to as many queries as possible (most of them irrelevant to the semantic content of the hub, which is freely chosen by the adversary). For example, in a text-to-image retrieval

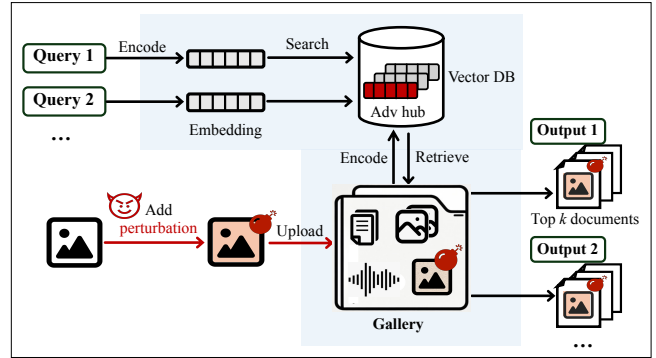


Figure 5: Attacking retrieval system with an adversarial hub.

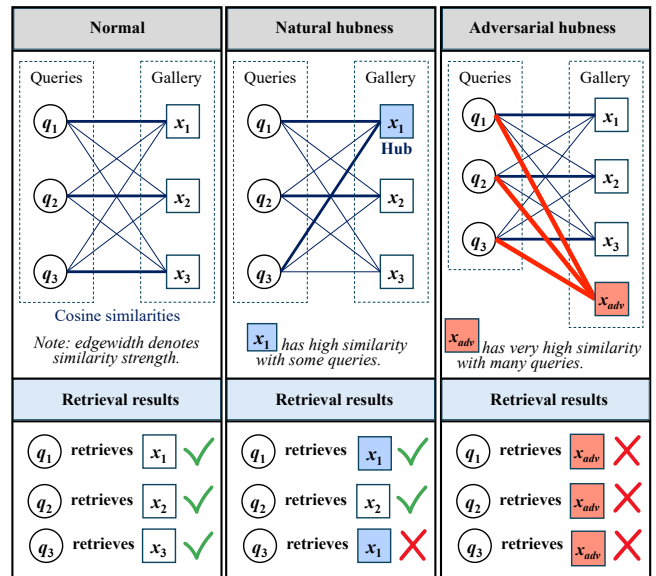


Figure 6: Natural hubs and adversarial hubs.

system, an adversarial image hub will be retrieved in response to captions such as “cars”, “food”, “house”, etc. In a text-to-audio retrieval system, regardless of what type of music the user searches for, the adversary’s audio will be retrieved as one of the most relevant songs. In this sense, adversarial hubs behave like natural hubs, except that they are retrieved much more frequently (see Figure 6).

Concept-Specific Objective. This attack is targeted: the attacker’s goal is to have their content retrieved only in response to queries related to a specific *concept* while avoiding retrieval for unrelated queries. This attack is more practical since it avoids spamming users with irrelevant results.

Since our experiment on concept-specific objectives primarily concerns text-to-image retrieval tasks, we define concepts in two ways: 1) Queries that contain specific, meaningful *keywords* aligned with the attacker’s interest. For example, an adversarial advertisement for a car dealership appear only when users search for “cars” or specific car models; and 2) Queries that form *clusters* in the

embedding space, where each cluster reflects high-level, abstract semantics of interest to the attacker. Such concepts are naturally captured by modern embedding models, which tend to group semantically similar inputs together. For example, a cluster may represent the concept of “outdoor adventure,” encompassing diverse queries like “mountain hiking,” “rock climbing,” and “camping under the stars.” Although these queries differ lexically, they are embedded closely together due to their shared semantic meaning. For modalities other than text, the keyword-based definition of a concept may not directly apply. However, the cluster-based definition can be naturally extended, as semantically similar inputs tend to form coherent clusters in the embedding space regardless of modality.

The concept-specific attack is superficially similar to attacks on retrieval-augmented generation (RAG) [10], which generates poisoned documents that are retrieved by queries with a certain trigger word. RAG attacks are currently limited to text-to-text retrieval and require poisoned documents to contain semantics-free gibberish whose embedding is close to the trigger. By contrast, our attack preserves the original semantics of the adversary’s content.

Security Consequences of Adversarial Hubness. Adversarial hubs can be used to spread spam, or simply to degrade performance of retrieval systems thus causing denial of service. For example, in the music industry [20, 29] platforms like Spotify [64] are constantly battling malicious actors who attempt to promote their content and manipulate platforms into streaming it for many users. In online retail, hubness attacks could manipulate product search. In social media, they could propagate misinformation and amplify misleading content. These examples show that adversaries today have an economic incentive to exploit hubness.

3.2 Attacker Knowledge and Capabilities

White-Box. In this setting, the attacker knows everything about the target system’s embedding models $\theta^{m_1}, \theta^{m_2}$, including architecture and parameters. He does not need to know anything about benign inputs in G (beyond basic information such as formatting) because adversarial hubs are independent of the existing gallery data points. He also does not need to know exact queries, since hubs are intended to work effectively across many different queries.

The white-box setting is realistic in several scenarios. First, many retrieval systems use publicly available pre-trained models (e.g., CLIP) with known architectures and parameters. Second, model extraction attacks can recover parameters of black-box models through repeated queries. Third, insider threats or data breaches could expose model details. The white-box setting follows Kerckhoffs’ principle [35]: security should not rely on the secrecy of the system but rather on its inherent robustness. This approach is standard in adversarial machine learning literature [46, 69].

Black-Box. Following the black-box adversarial examples literature [1, 42], we consider two black-box attack scenarios involving unknown target embedding models. In the *transfer attack*, the attacker has no API access to the embedding model or the retrieval system itself and must rely on a surrogate model to generate adversarial hubs that transfer to the unknown target. In the *query attack*, the attacker has API access to the embedding model used in the retrieval system and can issue a sequence of queries. Information

about the embedding models used by commercial systems is often available through public documentation. For instance, it is publicly known that Wayfair uses Google’s Vertex AI Embedding APIs to implement its search-by-image functionality [14]. These APIs of the embedding models return the embedding vector for a given input query, and such feedback enables the attacker to iteratively refine the generation of adversarial hubs.

Knowledge About Query Distribution. Generation of adversarial hubs requires some knowledge or assumptions about the queries. Even if the adversary does not know the true query distribution, they may still have meta-information (e.g., knowledge that the system accepts text queries to retrieve images, or even a few representative queries from the system demo). Therefore, we consider two levels of attacker knowledge: (1) *Exact Knowledge* of the true query distribution, and (2) *Proxy Knowledge* of a related but different query distribution. Proxy queries can be obtained from public benchmarks (e.g., text descriptions from MS COCO can approximate queries for a text-to-image retrieval system) and adjusted based on the available meta-information or example queries. For indiscriminate attacks, we consider both a small portion (0.4%) of exact knowledge in Section 5.1 and proxy knowledge in Section 7.3. For concept-specific attacks, the attacker selects the concept and constructs the corresponding queries (e.g., natural-language descriptions), thus he knows the query distribution he is targeting.

3.3 Generating Adversarial Hubs

We consider a cross-modal retrieval task where queries Q_t have modality m_1 and gallery data G have modality m_2 . The adversary’s goal is to generate an adversarial hub g_a in modality m_2 that is close to Q_t in the embedding space.

For the indiscriminate attack, Q_t contains 100 random samples from the query distribution. When this distribution is not known, Q_t is sampled from a proxy distribution. For the concept-specific attack, Q_t contains queries related to the (attacker-chosen) concept.

The attacker generates adversarial hubs by selecting an arbitrary initial input g_c in the same modality as the gallery G . This input g_c carries arbitrary semantic content (e.g., spam, product promotions, or audio clips) and is independent from existing gallery items and target queries Q_t . The attacker then introduces a bounded perturbation δ to produce an adversarial hub:

$$g_a = g_c + \delta, \quad \text{with constraint} \quad \|\delta\|_\infty \leq \epsilon. \quad (1)$$

The norm constraint on δ serves two primary purposes: (1) it ensures the adversarial input retains the attacker’s desired human-perceived semantics, preserving the integrity of visual, textual, or audio information (rational hub), and (2) it minimizes detectability by manual inspections or by end users, reducing the likelihood of the input appearing abnormal or suspicious [59]. If the attacker’s goal is simply to degrade the retrieval system’s performance (i.e., a “reckless” hub attack), this norm constraint can be removed entirely, resulting in a stronger, though potentially more noticeable, attack.

Simultaneously optimizing the adversarial hub against multiple query embeddings is computationally expensive when $|Q_t|$ is large. Instead, we compute a single representative centroid embedding of the target queries Q_t , which is the average of their cosine similarities. Formally, given the set of target query embeddings

$\{\theta^{m_1}(q) : q \in Q_t\}$, the centroid embedding c_t is defined as:

$$c_t = \frac{1}{|Q_t|} \sum_{q \in Q_t} \frac{\theta^{m_1}(q)}{\|\theta^{m_1}(q)\|}. \quad (2)$$

The attacker then solves the following constrained optimization problem to generate the adversarial hub embedding close to c_t .

$$\arg \min_{\delta} \mathcal{L}(g_a, c_t; \theta) = -\cos(\theta^{m_2}(g_c + \delta), c_t), \text{ s.t. } \|\delta\|_{\infty} \leq \epsilon. \quad (3)$$

Equation (3) is optimized via Projected Gradient Descent (PGD), which enforces the perturbation constraint through projection after each iteration [46]. In black-box settings where the target’s gradients are not available, we use the following two techniques.

Transfer Attack. We perform the white-box attack on a surrogate model θ^{m_1} and use the resulting adversarial hub against the black-box system. The surrogate can be a single embedding model or an ensemble of multiple, diverse models for better transferability [42, 65]. We consider an ensemble of K surrogates, denoted as $\Theta = \{\theta_i\}_{i=1}^K$ (we omit modality m_1 for clarity in presentation). For each surrogate θ_i , we compute its corresponding centroid embedding $c_{t,i}$ from the same Q_t , resulting in a set of centroids $C_t = \{c_{t,i}\}_{i=1}^K$. The importance of individual surrogates in the ensemble is quantified via weights $\lambda = \{\lambda_1, \lambda_2, \dots, \lambda_K\}$. The adversarial hub g_a is then generated by minimizing the following ensemble-based loss: $\mathcal{L}_T(g_a, C_t, \Theta) = \sum_{i=1}^K \lambda_i \cdot \mathcal{L}(g_a, c_{t,i}; \theta_i)$. For simplicity, we assign equal weights for each model as $\lambda_i = \frac{1}{K}$ in the transfer experiments in Section 7.1.

Query-Based Attack. In scenarios where the adversary does not have a surrogate but can continuously query the embedding model of the retrieval system, we adapt Square Attack [1], a state-of-the-art, query-efficient score-based black-box attack for generating adversarial examples. In the original Square Attack, the attacker’s objective is to maximize the likelihood of misclassification. We redefine it to maximize cosine similarity to the target embedding c_t , as shown in Eq. (3). This objective is optimized using an iterative, hierarchical random search process to improve query efficiency.

4 Experimental Setup

Datasets. We follow the prior literature on cross-modal retrieval [4]: for the text-to-image retrieval task, we use the standard MS COCO [11] dataset; for the image-to-image task, we use the CUB-200-2011 [71], and for the text-to-audio task, we use AudioCaps [36]. We also included MSR-VTT [78] to investigate the generalizability of adversarial hub across different query distributions.

MS COCO [11] is a widely used image captioning and text-to-image matching dataset. We use its test set of 5,000 images as the gallery and the associated 25,000 captions (5 each) as user queries.

CUB-200-2011 [71] is an image classification dataset consisting of various bird species. To form the gallery, we randomly select one test image from each of the 200 classes, and use the remaining 5,724 test images as user queries.

AudioCaps [36] is a widely used audio captioning dataset. We use its test set of 816 audios and corresponding text captions as the gallery and queries, respectively.

MSR-VTT [78] is a video captioning dataset containing approximately 10,000 video clips, each paired with on average 20 captions. For our query distribution generalization experiments, we treat MSR-VTT as a *proxy query distribution* and use the test split of 1,000 captions as simulated user queries to generate adversarial hubs. We then evaluate their effectiveness against the target MS COCO queries to assess cross-distribution generalization.

The query set Q_t used for adversarial hub generation is randomly sampled from either the original (target) or proxy query distributions, depending on the experiment. Unless otherwise stated, Q_t contains 100 queries for indiscriminate attacks and a variable number (greater than 20) for concept-specific attacks, depending on the concept. Each hub generation is repeated 100 times, and we report both the average and standard deviation.

Models. We use popular open-source encoders: ImageBind [22] (6 modalities), AudioCLIP [26] (3 modalities), and CLIP (2 modalities) [53]. For tasks involving images, we use a partially trained checkpoint of AudioCLIP, as it achieves better performance [26]. Our evaluations on CLIP are done on two architectures (ViT and ResNet-50) using the implementations provided by OpenCLIP [12].

Pinecone. In addition to “simulated” retrieval systems in prior work [4, 75], we evaluate a realistic setting using Pinecone’s image-to-image retrieval application.² Pinecone uses an unspecified version of CLIP [53] for its embeddings. We assume the adversary has access to common CLIP implementations but not the exact version (realistic since custom encoders are expensive) and can only upload gallery data without modifying configurations. We test on CUB-200-2011 using the same data split as before.

Attack Setup. To generate an adversarial hub, we randomly select a clean gallery point $g_c \in G$, optimize the perturbation δ based on Equation (3), and run PGD for $T = 1,000$ iterations to obtain $g_a = g_c + \delta$. We set the perturbation budget of δ as $\epsilon = 16/255$ for image and $\epsilon = 0.05$ for audio, following [85]. For the query attack, we set the query budget to 100,000, following the original paper [1]

Evaluation Metrics. We use two standard retrieval metrics, *Recall at Rank k* ($R@k$) and *Median Rank* (MdR).

Given a query $q_i \in Q = \{q_i\}_{i=1}^N$, we calculate the number of relevant documents in the gallery, R_i , and the number of relevant documents retrieved in the top- k list, R_i^k . Then $R@k$ is defined as $\frac{1}{N} \sum_{i=1}^N \frac{R_i^k}{R_i} \times 100\%$. Higher values indicate better retrieval performance. We report the results for different k . For the attack to be successful, the adversarial hub should appear in the top k retrieval results but not necessarily as the first result.

Let r_i be the rank of the first retrieved datum in the ranked list of all gallery items. Then, MdR is defined as $\text{median}(\{r_1, r_2, \dots, r_N\})$. Lower values indicate better retrieval performance.

For each evaluation experiment, we first measure the retrieval performance of user queries on the original *clean* gallery (clean retrieval performance). Next, we generate 100 adversarial hubs for images and audio and inject each hub into the gallery to create a *poisoned* gallery, then measure performance of both the injected hub and original, clean documents using the same set of queries.

²<https://github.com/pinecone-io/image-search-example>

An effective adversarial hub should achieve high $R@k$ and low MdR. We report the mean and standard deviation for both metrics.

5 Evaluation Without Defenses

We evaluate universal adversarial hubs in Section 5.1, compare with natural hubs in Section 5.2, then evaluate stealthy, word-based and cluster-based concept-specific hubs in Section 5.3.

5.1 Effectiveness of Universal Adversarial Hubs

Text-to-Image Retrieval. Table 1 presents text-to-image retrieval results across ImageBind, OpenCLIP, and AudioCLIP models on MS COCO. On clean gallery data, model performance varies from $R@10 = 81.1\%$ and $\text{MdR} = 2$ for OpenCLIP-ViT to $R@10 = 50.7\%$ and $\text{MdR} = 10$ for AudioCLIP.

When an adversarial hub is introduced, it is consistently retrieved by many irrelevant queries. OpenCLIP-RN50 is the most vulnerable, with $R@1 = 97.6\%$ for the adversarial hub. AudioCLIP is more robust, yet $R@1 = 62.0\%$. For all models except AudioCLIP, the adversarial hub achieves $\text{MdR} = 1$, i.e., it is ranked as most relevant even though it is semantically unrelated to the queries. The partially-trained AudioCLIP is more robust but its poor performance on the clean gallery ($R@1 = 18.8\%$) makes it unusable in practice.

Retrieval performance on clean gallery data drops slightly if an adversarial hub is present. For example, ImageBind achieves $R@10 = 79.8\%$ for clean gallery points in presence of an adversarial hub, vs. 81.0% without the hub. This shows that relevant gallery points are still retrieved alongside the adversarial hub, which is unsurprising since the hub is a single point. The low median rank (typically 1) and the increasing $R@k$ at larger k indicate that the adversarial hub primarily affects the top ranks, while largely preserving retrieval quality across the rest of the gallery.

Our adversarial hubs exhibit *good generalization*. They are optimized on only 100 random text queries from MS COCO, yet achieve high recall rates on the full test set of 25,000 captions. This indicates the adversarial hubs exploit inherent vulnerabilities in the embedding space (rather than overfitting to specific queries) and broadly effective against any user queries from the same distribution.

Text-to-Audio Retrieval. Table 2 presents text-to-audio retrieval results on the AudioCaps dataset. Our adversarial hubs achieve $R@1$ over 50% and $R@10$ as high as 81.3% for ImageBind and 85.8% for AudioCLIP. The median rank for adversarial hubs is approximately 1.5, indicating their high “relevance” as it appears to users.

These results show that a single adversarial audio can align with a broad range of captions. Although text-to-audio retrieval is slightly more robust than text-to-image, it is still vulnerable to adversarial manipulation. This demonstrates that cross-modal hubness extends beyond the (well-studied) image domain to audio representations, and likely to other modalities as well. Overall, the vulnerability appears to be an intrinsic property of multi-modal embedding spaces, rather than a feature of any specific modality.

Image-to-Image Retrieval. Our primary focus is cross-modal retrieval, but our attack also potentially affects embedding-based “search by image” systems. Table 3 presents image-to-image retrieval results on the CUB-200-2011 dataset, using the same models

as above. In Section 7.1, we apply the attack to a black-box system from a Pinecone tutorial.

Image-to-image retrieval is more robust than text-to-image but adversarial hubs are still retrieved among the top results for multiple queries. For OpenCLIP-ViT, $R@1 = 4.1\%$ but $R@10 = 90.7\%$. Similarly, for ImageBind, $R@1 = 5.5\%$ but $R@10 = 87.7\%$.

We conjecture that image-to-image retrieval resists adversarial hubs better than cross-modal retrieval because embeddings cluster based on modality. Retrieval is based on relative similarity. In ImageBind, cosine similarity between a random text and all other texts is 0.2185; for images, average similarity is 0.2916, indicating similar concentration within each modality. But average similarity between a random image and all texts is only 0.0139. Therefore, the same absolute level of similarity that is sufficient to make a hub most relevant for queries from another modality may not be sufficient to make it most relevant for queries from the same modality.

Furthermore, in ImageBind the center of all text query embeddings has an average cosine similarity of 0.454 with the individual queries. By contrast, average similarity between images and their ground-truth text captions is 0.311. Aligning an image with this center achieves average cosine similarity of 0.392 with text queries and thus turns it into a hub because, on average, it is closer to the queries than clean images are to their correct captions.

In summary, adversarial hubs can effectively exploit modality gaps in embedding spaces. A similar observation was made in [40]: natural hubness affects cross-modal retrieval more than uni-modal. Single-modality representations tend to be more compact potentially reducing vulnerability to both natural and adversarial hubs.

5.2 Comparing Adversarial and Natural Hubs

Figure 7 shows the number of gallery points retrieved as the most relevant for different numbers of queries (y-axis) across text-to-image, image-to-image, and text-to-audio retrieval tasks. For a given y , width indicates the number of points retrieved y times. The adversarial hub (in red) is retrieved as the most relevant gallery point an order of magnitude more frequently than any natural hub. On the MS COCO dataset with ImageBind embeddings, our adversarial hub was retrieved as the most relevant 21,136 times, compared to 102 times for the most common natural hub—a $\times 207$ increase. The retrieval frequency gap is smallest for the CUB-200-2011 dataset with OpenCLIP-ViT ($\times 1.9$).

The correct metric for a natural hub is the number of *irrelevant* queries for which it is retrieved. In CUB-200-2011 using OpenCLIP-ViT (where the gap between natural and adversarial hubs is the smallest), a natural hub is, on average, relevant to 28 user queries. Even though some clean gallery points are classified as natural hubs because they are retrieved by up to 100 queries, the actual number of irrelevant retrievals is only $100 - 28 = 72$.

5.3 Concept-Specific Adversarial Hubs

We evaluate stealthy hubs for word- and cluster-based concepts on ImageBind embeddings and MS COCO dataset.

Generation of Concept-Specific Hubs. To create word-based concepts, we extracted 100 distinctive words representing visual concepts from the MS COCO test set using ChatGPT [49], excluding common function words (e.g., “be”, “of”, “in”) and terms with limited

Table 1: Result for text-to-image retrieval (MS COCO). “Clean” denotes the original gallery, “Poisoned” denotes the gallery with an adversarial hub. “Relevant Doc.” is the documents relevant to the query, “Adv. Hub.” is the adversarial hub. Attack performance is shaded. Results show mean and standard deviation across 100 independently generated adversarial hubs. See Section 4 for detailed description of metrics and evaluation methodology.

Model	Gallery	Retrieved	$R@1$ (%) \uparrow	$R@5$ (%) \uparrow	$R@10$ (%) \uparrow	MdR \downarrow
ImageBind	Clean	Relevant Doc.	48.4	72.7	81.0	2.0
	Poisoned	Relevant Doc.	10.9 \pm 2.0	69.6 \pm 0.0	79.8 \pm 0.0	2.9 \pm 0.1
	Poisoned	Adv. Hub	85.1 \pm 3.1	98.1 \pm 0.7	99.0 \pm 0.4	1.0 \pm 0.0
AudioCLIP	Clean	Relevant Doc.	18.8	39.5	50.7	10.0
	Poisoned	Relevant Doc.	8.8 \pm 3.5	36.9 \pm 0.4	49.3 \pm 0.2	11.0 \pm 0.0
	Poisoned	Adv. Hub	62.0 \pm 18.7	81.4 \pm 13.3	87.5 \pm 10.4	1.6 \pm 1.4
OpenCLIP-ViT	Clean	Relevant Doc.	48.5	72.8	81.1	2.0
	Poisoned	Relevant Doc.	11.3 \pm 2.2	69.8 \pm 0.0	79.9 \pm 0.0	3.0 \pm 0.1
	Poisoned	Adv. Hub	84.4 \pm 3.5	97.9 \pm 0.8	98.9 \pm 0.5	1.0 \pm 1.0
OpenCLIP-RN50	Clean	Relevant Doc.	28.3	53.0	64.1	5.0
	Poisoned	Relevant Doc.	1.4 \pm 0.8	49.8 \pm 0.0	62.2 \pm 0.0	6.0 \pm 0.0
	Poisoned	Adv. Hub	97.6 \pm 1.6	99.5 \pm 0.5	99.7 \pm 0.3	1.0 \pm 0.0

Table 2: Text-to-audio retrieval (AudioCaps).

Model	Gallery	Retrieved	$R@1$ (%) \uparrow	$R@5$ (%) \uparrow	$R@10$ (%) \uparrow	MdR \downarrow
ImageBind	Clean	Relevant Doc.	10.6 \pm 0.0	30.7 \pm 0.0	43.7 \pm 0.0	13.0 \pm 0.0
	Poisoned	Relevant Doc.	7.3 \pm 0.6	27.4 \pm 0.3	40.5 \pm 0.1	16.0 \pm 0.0
	Poisoned	Adv. Hub	52.2 \pm 6.7	71.2 \pm 5.6	81.3 \pm 4.8	1.5 \pm 0.7
AudioCLIP	Clean	Relevant Doc.	6.2 \pm 0.0	20.7 \pm 0.0	31.8 \pm 0.0	27.0 \pm 0.0
	Poisoned	Relevant Doc.	2.5 \pm 0.8	18.8 \pm 0.3	30.6 \pm 0.2	28.0 \pm 0.0
	Poisoned	Adv. Hub	58.0 \pm 13.7	77.6 \pm 10.5	85.8 \pm 7.9	1.5 \pm 0.9

Table 3: Image-to-image retrieval (CUB-200-2011).

Model	Gallery	Retrieved	$R@1$ (%) \uparrow	$R@3$ (%) \uparrow	$R@5$ (%) \uparrow	$R@10$ (%) \uparrow	MdR \downarrow
ImageBind	Clean	Relevant Doc.	59.2	77.7	84.9	92.3	1.0
	Poisoned	Relevant Doc.	55.7 \pm 0.2	75.5 \pm 0.1	83.2 \pm 0.1	91.0 \pm 0.0	1.0 \pm 0.0
	Poisoned	Adv. Hub	5.5 \pm 0.7	39.5 \pm 2.6	62.2 \pm 2.5	87.7 \pm 2.0	4.2 \pm 0.4
AudioCLIP	Clean	Relevant Doc.	12.1	22.2	28.3	38.9	19.0
	Poisoned	Relevant Doc.	11.0 \pm 0.5	21.6 \pm 0.5	27.9 \pm 0.4	39.2 \pm 0.2	18.0 \pm 0.0
	Poisoned	Adv. Hub	13.3 \pm 6.1	31.6 \pm 11.1	44.8 \pm 12.9	66.7 \pm 13.1	6.8 \pm 3.1
OpenCLIP-ViT	Clean	Relevant Doc.	59.5	79.5	86.2	93.0	1.0
	Poisoned	Relevant Doc.	56.6 \pm 0.2	77.2 \pm 0.2	84.4 \pm 0.1	92.6 \pm 0.1	1.0 \pm 0.0
	Poisoned	Adv. Hub	4.1 \pm 0.6	34.6 \pm 2.7	61.0 \pm 3.1	90.7 \pm 2.6	4.7 \pm 0.5
OpenCLIP-RN50	Clean	Relevant Doc.	22.0	38.7	48.0	62.1	6.0
	Poisoned	Relevant Doc.	20.5 \pm 0.4	36.6 \pm 0.3	46.4 \pm 0.1	60.8 \pm 0.1	6.6 \pm 0.5
	Poisoned	Adv. Hub	20.0 \pm 2.8	45.7 \pm 4.0	59.4 \pm 3.7	77.7 \pm 2.9	4.1 \pm 0.6

visual representational value (e.g., “play”, “shape”). For each concept word, the query set Q_t is all queries containing that word.

To create cluster-based concepts, we partitioned 25,000 queries into 1,000 clusters using K -means clustering in the embedding space

(this technique was previously used to define subpopulations for data poisoning [31, 66]). Each cluster reflects a semantic concept (e.g., outdoor adventures) even if the queries are not lexically related (e.g., “mountain climbing”, “camping under the stars”).

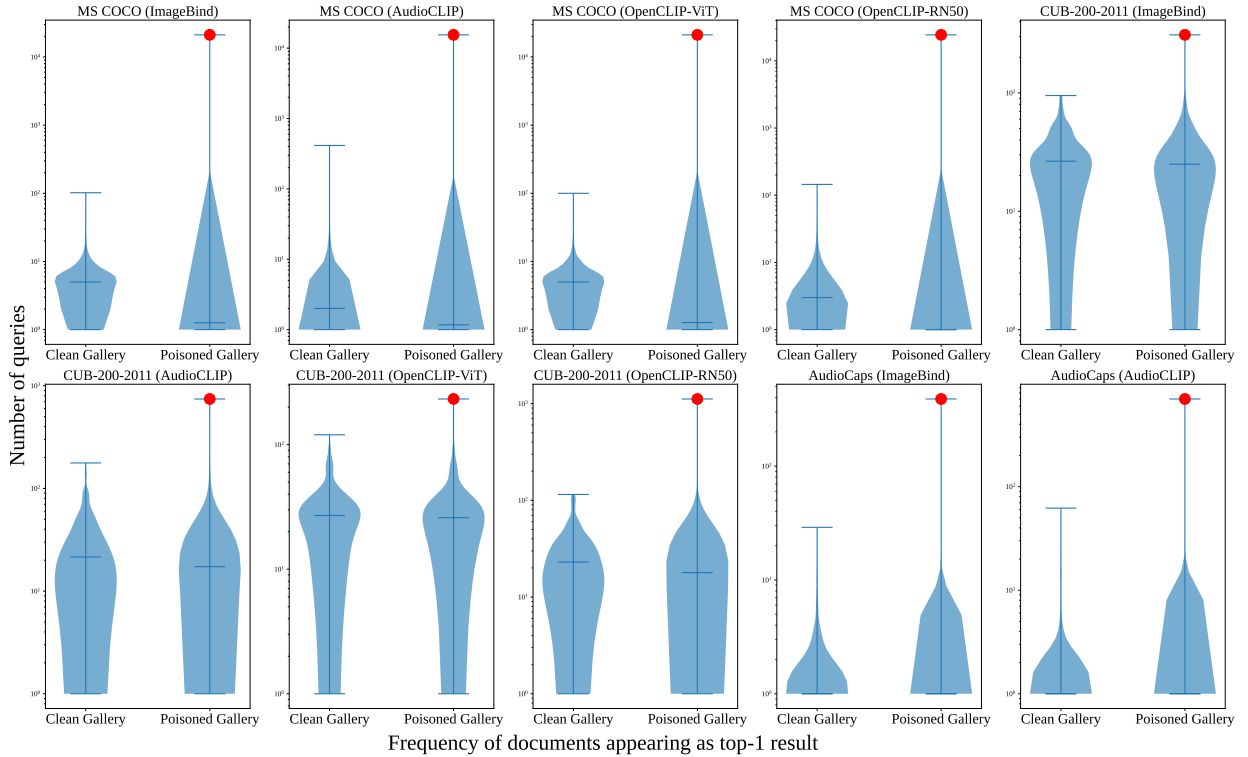


Figure 7: Retrieval frequency of adversarial and natural hubs. Adversarial hubs (red dots) are retrieved significantly more frequently than natural hubs. Plot width indicates retrieval frequency (log scale), with results averaged over 100 trials.

Generation of both word-based and cluster-based concept-specific adversarial hubs follows the optimization procedure from Equation (2), differing only in the choice of the target query set Q_t and the random initial image. We evaluate attack effectiveness using (1) retrieval performance on the intended concept-specific queries (higher is better), and (2) collateral damage, defined as retrieval performance on unrelated queries (lower is better). This setup simulates a realistic scenario where an adversary wants their hub to be frequently retrieved for queries related to the target concept while remaining largely invisible (and thus stealthy) to unrelated queries.

Effectiveness and Stealthiness of Word- and Cluster-Based Hubs. Table 4 presents the results for word-based and cluster-based concept-specific adversarial hubs. Word-based hubs achieve $R@1 = 28.6\%$ and $R@10 = 61.7\%$. These metrics are almost 100% for cluster-based hubs, demonstrating that the attack is more effective when target queries share high-level semantics.

To assess stealthiness, we measure retrieval performance of concept-specific hubs on unrelated queries (the vast majority of the 25,000 text queries). Word-based hubs are almost never retrieved ($R@10 \leq 0.7\%$). Retrieval rates for unrelated queries are slightly higher for cluster-based hubs, 8.6% at $R@1$ and 18.4% at $R@10$, indicating a modest trade-off between effectiveness and stealthiness. Future work can explore more refined hub generation methods to better balance effectiveness and stealthiness.

In Section 6, we show that defenses for natural hubs are much less effective against concept-based adversarial hubs.

6 Evaluation of Defenses

In Section 6.1, we outline a representative defense against natural hubs [4], then evaluate its effectiveness against adversarial hubs in Section 6.2. In Section 6.3, we discuss potential adaptations of defenses against adversarial examples to mitigate adversarial hubs.

6.1 Querybank Normalization (QB-Norm)

Defense Mechanism. This defense [4] normalizes abnormally high similarity scores in cross-modal retrieval. It employs a query bank Q_b of typical user queries and creates an activation set with the indices of gallery points that appear at least once in the top- k results for the queries in Q_b :

$$\mathcal{A} = \{j : j \in \operatorname{argmax}_{g_j \in G}^k \operatorname{sim}(q_i, g_j), q_i \in Q_b\}$$

For each gallery point g_j , a precomputed probe vector $p_j \in \mathbb{R}^K$ contains its similarities with K most relevant queries from Q_b .

When processing a user query q , if the index of the most relevant gallery point is in \mathcal{A} , its similarity score $\eta_q(j)$ is normalized:

$$\eta_q(j) = \begin{cases} \frac{\exp(\beta \cdot \operatorname{sim}_j)}{1^T \exp([\beta \cdot p_j])} & \text{if } \operatorname{argmax}_{g_j \in G} \operatorname{sim}_j \in \mathcal{A} \\ \operatorname{sim}_j & \text{otherwise} \end{cases} \quad (4)$$

Table 4: Concept-specific adversarial hubs on MS COCO with and without QB-Norm defense. Performance is reported on poisoned galleries using *Original* and *Targeted* query sets. Standard deviations omitted for concept-specific hubs due to evaluation on heterogeneous query subsets.

QB-Norm	Retrieved	Query	R@1 (%)	R@5 (%)	R@10 (%)	MdR
No	Relevant Doc.	Original	10.9 \pm 2.0	69.6 \pm 0.0	79.8 \pm 0.0	2.9 \pm 0.1
	Universal Hub	Original	85.1 \pm 3.1	98.1 \pm 0.7	99.0 \pm 0.4	1.0 \pm 0.0
	Word-based Concept-specific Hub	Original	0.2	0.4	0.7	912.1
	Word-based Concept-specific Hub	Targeted	28.6	53.5	61.7	50.8
	Cluster-based Concept-specific Hub	Original	8.6	15.0	18.4	24.1
	Cluster-based Concept-specific Hub	Targeted	100.0	100.0	100.0	1.0
Yes	Relevant Doc.	Original	49.7 \pm 0.0	74.1 \pm 0.1	82.6 \pm 0.1	2.0 \pm 0.0
	Universal Hub	Original	0.0 \pm 0.0	11.5 \pm 2.4	12.2 \pm 2.7	699.9 \pm 72.8
	Word-based Concept-specific Hub	Original	0.0	0.2	0.3	1379.2
	Word-based Concept-specific Hub	Targeted	22.9	44.6	53.6	55.5
	Cluster-based Concept-specific Hub	Original	0.1	5.1	7.6	4015.7
	Cluster-based Concept-specific Hub	Targeted	95.3	98.3	99.0	1.0

where β is a temperature parameter controlling normalization strength. We focus on this defense because it is the first scalable solution that minimizes impact on retrieval performance while mitigating natural hubs in for modern cross-modal retrieval systems. Subsequent approaches [13, 75] follow similar architectures with minor variations in the query bank construction. For our evaluation, we use the default hyperparameters from the original paper [4].

Lazy vs. Diligent Defense Implementation. Querybank normalization is very expensive for large-scale retrieval systems with continuously updated galleries because activation sets and probe vectors must be re-computed for every gallery update. We call this the *diligent* defense. An alternative is the *lazy* defense which does these computations periodically, not every time a new point is added. Lazy defense has a vulnerability window: if an adversary adds an adversarial hub, the system will not be defended against this hub until the next update because the hub will not be in the activation set \mathcal{A} and its probe vector p_j will be zero. In our evaluation, we consider the stronger, diligent defense, even though it is computationally prohibitive in real-world deployments.

6.2 Effectiveness of QB-Norm

Universal Hubs. We evaluate the effectiveness of the QB-Norm defense on MS COCO with ImageBind embedding. Without adversarial hubs, it slightly improves retrieval performance by mitigating (rare) natural hubs: $R@1$ increases from 48.4% to 49.9%.

Table 4 shows that QB-Norm is effective against universal adversarial hubs, reducing their $R@1$ of adversarial hubs drops from 85.1% to 0% and increasing median rank from 1 to 700. Retrieval accuracy for relevant documents in the presence of adversarial hubs increases 10.9% to 49.7%, and median rank increases from 2.9 to 2.0.

In practice, the key challenge for this defense is its cost. It must maintain a comprehensive query bank Q_b that is representative of potential user queries, which potentially requires millions or

billions of queries. Furthermore, activation sets and probe vectors must be frequently re-computed for the entire gallery. Using a small subset, such as the k -nearest neighbors of gallery data points in Q_b [13], increases the speed of this defense by over 100x, but introduces exploitable gaps due to the inherent *asymmetry* between the top- k samples in Q_b and the actual target queries Q_t (which corresponds to Q in our indiscriminate attack setting).

To illustrate this, we evaluate the same universal hubs against the compute-efficient variant [13] and observe a $R@1 = 3.3\%$ and $R@10 = 45.2\%$, in contrast to $R@1 = 0\%$ and $R@10 = 12.2\%$ achieved against the naive QB-norm defense. These results show a clear trade-off between computational efficiency and effectiveness of this defense even when adversarial hubs are universal and non-adaptive. We expect that an adaptive attacker could achieve even higher $R@k$ performance, but leave it for future work.

Next, we show how concept-specific hubs *naturally* exploit the “asymmetry” between Q_b and Q_t to evade this defense.

Concept-Specific Hubs. Table 4 shows that $R@1$ of word-specific hubs by their targeted queries decreases only marginally (by 5.7%) in the presence of QB-Norm. Cluster-specific hubs remain highly effective, too, achieving 95.3% $R@1$ and a median rank of 1 for their corresponding queries. Collateral damage (i.e., retrieval by unrelated queries) is minimal for both types of concept-specific hubs. Concept-specific hubs successfully evade the defense because their target query distribution Q_t differs significantly from the typical queries Q_b used by QB-Norm for normalization.

In summary, universal adversarial hubs are useful for benchmarking adversarial robustness of retrieval systems but they are more likely to be detected than stealthy, concept-specific hubs.

6.3 Adapting Adversarial Examples Defenses

Some defenses are based on input processing, such as JPEG compression [25], feature distillation [43] and feature squeezing [79].

Table 5: Black-box attack performance in text-to-image retrieval (MS COCO). Results show effectiveness of transfer-based and query-based attacks across different models.

Target Model	Attack Method	R@1(%) \uparrow	R@5(%) \uparrow	R@10(%) \uparrow	MdR \downarrow
ImageBind	Transfer	76.9 \pm 5.2	96.6 \pm 1.3	98.2 \pm 0.8	1.0 \pm 0.0
	Query-based	0.7 \pm 1.1	8.1 \pm 9.7	15.2 \pm 16.1	120.5 \pm 129.2
AudioCLIP	Transfer	0.2 \pm 0.2	0.6 \pm 0.5	1.1 \pm 0.9	596.6 \pm 266.1
	Query-based	4.6 \pm 3.7	14.9 \pm 8.7	22.9 \pm 11.5	60.5 \pm 59.7
OpenCLIP-ViT	Transfer	76.2 \pm 6.5	96.4 \pm 0.8	98.1 \pm 0.1	1.0 \pm 0.0
	Query-based	0.7 \pm 1.1	8.4 \pm 1.0	15.7 \pm 16.3	115.4 \pm 137.3
OpenCLIP-RN50	Transfer	0.1 \pm 0.2	0.4 \pm 0.4	0.7 \pm 0.7	764.3 \pm 459.8
	Query-based	5.0 \pm 3.9	15.6 \pm 8.1	23.4 \pm 9.9	42.2 \pm 25.2

These defenses have a significant negative impact on clean performance, not only for classification tasks [25, 79] but also for retrieval. For example, in our text-to-image retrieval on MS COCO, common input transformations (JPEG compression, Gaussian blur, random affine transformations, color jitter, random horizontal flips, and perspective changes) reduce the $R@1$ across all embedding models by an average of 14.1%. In contrast, query normalization tends to improve clean performance. Furthermore, these defenses fail against adaptive attacks [2, 28, 62]. A detailed exploration of these defenses and the arms race with adaptive attacks is beyond the scope of this paper and left for future work.

Another line of defense focuses on designing robust models, either through adversarial training [46, 84] or certifiable methods [15, 24, 76]. However, these approaches face serious challenges in modern retrieval systems due to limited scalability and poor performance on large models. Unlike adversarial examples, which are mostly demonstrated on toy datasets like CIFAR-10 [38], retrieval tasks involve high-resolution natural images and significantly larger models. In addition to scalability challenges, retrieval tasks inherently involve a robustness-invariance tradeoff [70]: models need a certain degree of sensitivity to enable improved retrieval (i.e., distinguishing different clean inputs), but the same sensitivity can be deliberately exploited by attackers to generate adversarial hubs. It is thus difficult to determine which inputs should or should not be aligned in the embedding space during robust training.

7 Relaxing Attack Assumptions

Although our main goal is to benchmark adversarial robustness of cross-modal retrieval systems in white-box settings, which is consistent with prior adversarial examples literature [2, 8], in practical applications attackers may not always have access to the target system’s embedding model or query distribution. We now show that our adversarial hubs remain effective even when attackers only have limited knowledge about the target embedding model (Section 7.1) and the target query distribution (Section 7.2).

7.1 Black-Box Universal Adversarial Hubs

In this section, we investigate how to generate adversarial hubs with a limited knowledge of the target embedding model.

Transfer Attack. We first consider attackers who use available open-source embedding models as surrogates to create adversarial hubs that transfer to the black-box target system without additional queries to the latter. From our four models (ImageBind, AudioCLIP, OpenCLIP-ViT, OpenCLIP-ResNet-50), we select three as the adversary’s local model ensemble and treat the remaining one as the black-box target (we omit the results using individual models as surrogates because ensembles work better). Table 5 shows that our transfer attack achieves varying degrees of success against different targets. It is highly effective against ImageBind and OpenCLIP-ViT, achieving an average top-1 recall of $R@1 = 76.5\%$ and a median rank of $MdR = 1.0$. Since ImageBind extends OpenCLIP-ViT’s architecture by incorporating additional modalities while preserving the core visual encoder, including OpenCLIP-ViT in the surrogate ensemble enhances transferability to ImageBind, and vice versa. Our adversarial hubs show limited transferability to OpenCLIP-RN50 and AudioCLIP, with an average top-1 recall of $R@1 = 0.15\%$ and $MdR = 680.4$, though still better than random chance $R@1 = 0.02\%$ and $MdR = 2500$. We find that our transfer technique pushes the embedding of the adversarial hub close to the centroid of queries in the embedding space of the target model but this proximity is insufficient for the hub to become the nearest neighbor of many unrelated queries that contribute to the centroid.

These results indicate that architectural similarity between the surrogates and targets is a critical factor in transfer attack success. This matches prior findings on multi-modal adversarial alignment [85], where adversarial examples transfer well within similar architectures but poorly to very different ones. There are only a few popular visual and audio encoders, making it possible for an adversary to make educated guesses about the architecture of the target system and include similar models in their surrogate ensemble. Developing transfer techniques with better cross-architecture generalizability remains an open challenge for future research.

Pinecone. In addition to academic benchmarks, we evaluate our black-box attack on a image-to-image retrieval system implemented by Pinecone, a commercial vector database. We use the OpenCLIP-ViT embedding as the local surrogate and target image-to-image retrieval, reporting the results for $k \leq 5$ per this system’s default

Table 6: Pinecone image-to-image retrieval (CUB-200-2011).

Model	Gallery	Retrieved	$R@1(\%)\uparrow$	$R@3(\%)\uparrow$	$R@5(\%)\uparrow$
Pinecone	Clean	Relevant Doc.	25.4	43.0	52.7
	Poisoned	Relevant Doc.	24.5 \pm 0.2	41.9 \pm 0.6	51.8 \pm 0.7
	Poisoned	Adv. Hub	7.5 \pm 1.5	21.4 \pm 3.5	31.7 \pm 4.5

Table 7: Effectiveness of adversarial hubs across different query distributions. Results show attack performance when using queries from alternative datasets (rows) to generate hubs that target MS COCO.

Target Dataset	$R@1(\%)\uparrow$	$R@5(\%)\uparrow$	$R@10(\%)\uparrow$	MdR \downarrow
CUB-200	4.8 \pm 1.8	15.1 \pm 3.9	23.0 \pm 5.2	42.4 \pm 12.5
AudioCaps	10.6 \pm 2.8	30.8 \pm 5.8	41.9 \pm 6.7	17.0 \pm 6.3
MSR-VTT	35.8 \pm 6.4	66.4 \pm 8.2	76.8 \pm 7.6	2.7 \pm 1.3

setup. Table 6 shows that our attack achieves $R@1 = 7.5\%$ and $R@5 = 31.7$, comparable to the simulated settings in Section 5.1.

Query-Based Attack. We also evaluate query-based attacks, where adversaries submit multiple API queries to the black-box embedding models used in the target retrieval system and iteratively refine adversarial hubs. For these attacks, we run our adapted Square Attack with 100,000 queries. Although less effective than white-box techniques or the most successful transfer attacks, this approach remains effective across all tested models without requiring knowledge of the target’s model architecture. The query-based attack performs best against OpenCLIP-RN50, achieving 23.4% top-10 recall and median rank of 42.2. Future work could explore reducing the query budget and developing more effective black-box optimization techniques, or even adopting hybrid strategies by combining with transfer attacks [65].

7.2 Different Query Distributions

We evaluate generalizability of our adversarial hubs across different query distributions by using text queries from other datasets (CUB-200, AudioCaps, MSR-VTT) to generate hubs for the text queries from MS COCO. Table 7 shows that the attack remains effective. MSR-VTT yields the strongest transfer performance ($R@1 = 35.8\%$, $R@10 = 76.8\%$), likely because its visual-linguistic properties are similar to MS COCO and the attack only needs to approximate common visual concepts (e.g., objects and scenes) rather than match the exact query distribution. Hubs optimized for CUB-200 exhibit the weakest transfer performance ($R@1 = 4.8\%$), which is expected given this dataset focuses on fine-grained object categories rather than descriptive captions. AudioCaps results are in the middle ($R@1 = 10.6\%$), demonstrating our attack’s ability to exploit cross-modal semantic relationships despite significant modality differences. These findings indicate that our approach is robust to differences and shifts in query distributions.

7.3 Ablation Studies

We conduct additional ablation studies to assess the impact of the target query distribution size ($|Q_t|$) and the perturbation budget (ϵ)

Table 8: Impact of perturbation bound ϵ on attack performance. Results show how different perturbation magnitudes affect the retrieval metrics for adversarial hubs generated with ImageBind on MS COCO dataset.

ϵ	$R@1(\%)\uparrow$	$R@5(\%)\uparrow$	$R@10(\%)\uparrow$	MdR \downarrow
8/255	62.8 \pm 10.7	92.9 \pm 4.4	96.4 \pm 2.4	1.1 \pm 0.4
16/255	85.1 \pm 3.1	98.1 \pm 0.7	99.0 \pm 0.4	1.0 \pm 0.0
32/255	90.5 \pm 1.4	98.8 \pm 0.3	99.4 \pm 0.2	1.0 \pm 0.0
64/255	91.5 \pm 1.1	99.0 \pm 0.3	99.5 \pm 0.2	1.0 \pm 0.0

on adversarial hub performance in text-to-image retrieval tasks on the MS COCO dataset.

Different Sizes of Target Query Set Q_t . The x -axis in Figure 8 denotes different sizes of the target query set Q_t . Note that the default size of Q_t used in our main experiments (Section 5–Section 7) is 100. The left y -axis shows the top-1 retrieval rate of adversarial hubs, each generated using a different Q_t , evaluated against the 25,000 test queries. The right y -axis shows the average cosine similarity between the embeddings of these test queries and the corresponding adversarial hubs.

The solid lines in the figure represent the performance of our optimized attack based on Equation (3) across varying $|Q_t|$. The dotted lines indicate the performance of a “hypothetical” optimal attack, where the adversarial hub embedding exactly matches the centroid \mathbf{c}_t of Q_t . This serves as an upper bound on both top-1 recall and average cosine similarity, since actual attacks may not perfectly align with \mathbf{c}_t .

From the figure, we observe that for both metrics, the solid and dotted lines increase with larger $|Q_t|$. However, the top-1 recall saturates around 85.1% when Q_t contains just 100 samples. Further increasing $|Q_t|$ yields only marginal gains. This suggests that adversarial hubs can be effectively generated using a relatively small set of queries (e.g., 0.4% of the 25,000 total queries), while still closely approximating the embedding distribution of a much larger set. The diminishing returns beyond this saturation point are likely due to the compactness of the query embedding space, allowing 100 samples to provide a strong approximation, which our optimization method (Equation (3)) effectively exploits.

Different Perturbation Bound. Table 8 shows how the perturbation bound ϵ influences attack performance under the optimization in Equation (3). Even small perturbations ($\epsilon = 8/255$) achieve notable effectiveness with 62.8% $R@1$. Our default setting ($\epsilon = 16/255$), commonly used for generating adversarial examples, achieves 85.1% $R@1$ with MdR = 1.0, striking a strong balance between attack success and imperceptibility. Larger bounds ($\epsilon = 32/255$, $64/255$) yield only marginal gains (90.5% and 91.5% $R@1$, respectively), indicating diminishing returns. This suggests that increasing the perturbation magnitude primarily raises detection risk without meaningful performance improvement, validating our chosen ϵ as an effective trade-off between effectiveness and stealthiness.

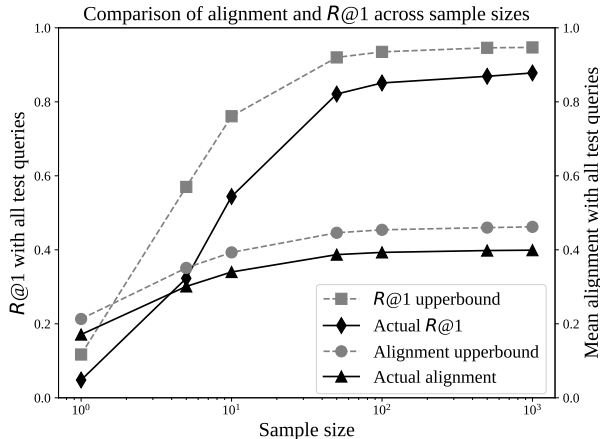


Figure 8: Performance vs. sample size. Attack success rate (ASR) and cosine similarity between adversarial hub and query embeddings improve with larger target sample sizes, converging at around 100 samples.

8 Related Work

Adversarial Alignment and Adversarial Examples. The most relevant related work investigates *adversarial alignment* of inputs in multi-modal embedding spaces [19, 85]. These attacks incrementally adjust a malicious input to align with a *single* target embedding in an arbitrary modality. In contrast, adversarial hubs achieve the harder goal of aligning a single input to a *large number* of target embeddings in arbitrary modalities.

Our work builds on the broader literature on *untargeted* and *targeted* adversarial examples. Untargeted attacks cause outputs that are incorrect but not controlled by the adversary [23], while targeted attacks induce a specific, adversary-chosen, incorrect output [9]. In contrast, our approach seeks to generate adversarial inputs that work for *multiple targets at once* (dozens of thousands of queries in the case of multi-modal retrieval).

In this space, the most closely related papers are adversarial cross-modal examples [18, 21, 50, 61, 77, 87]. As well as being task-specific, these techniques only attack single targets. In other recent work [7, 52, 86], untargeted adversarial perturbations are used for jailbreaking and prompt injection in multi-modal chatbots.

Hoedt et al. [29] create unimodal audio adversarial hubs for multiple targets in audio-to-audio retrieval, but the attack is limited to a handful of samples. Other unimodal adversarial examples against specific downstream tasks include toxicity classification [30], reading comprehension [34], and chatbots [90]. Untargeted adversarial perturbations against contrastively-trained encoders are demonstrated in [37, 81, 89].

Importantly, unlike prior multi-target attacks, which induce different incorrect outputs for the same input across multiple models [39], and universal adversarial perturbations [47], which generalize across inputs rather than targets, our method operates against a single model but generalizes across embedding targets.

Poisoning Retrieval-Augmented Generation. Our work is also closely related to retrieval-augmented generation (RAG) poisoning, which involves an adversary who designs and injects adversarial documents into a RAG system’s corpus. In this setting, adversaries create documents that have two goals: (1) they are frequently retrieved (retrieval poisoning) and (2) they result in unsafe generations when retrieved (generation poisoning).

Chaudhari et al. [10] study trigger-based retrieval poisoning: they create adversarial documents that are retrieved for any query containing a specific trigger word. Others [80, 88] study triggerless retrieval poisoning attacks by clustering clean documents and generating an adversarial document for each cluster. Zhang et al. [83] introducing a method to produce natural-looking text that works for both trigger-based and triggerless attacks. After they are retrieved, adversarial documents cause generative models to produce harmful content or suppress correct answers [10, 60].

Unlike our work, these approaches work with pure text-to-text retrieval systems. While our work is more closely related to retrieval poisoning, an adversary could also target generation in *any modality* by including malicious generation targets in their query set Q_t . We leave this for future work.

Mitigation of Natural Hubness. Since hubs occur organically, without adversarial manipulation, in high-dimensional distributions, prior work focused on mitigating *natural hubness*. There are train-time [41] and post-processing methods [4, 57, 67, 75] for mitigating natural hubs.

Train-time methods rely on hubness-aware loss functions [41] which downweigh points that are close to multiple neighbors. While effective, these methods are costly for large models and have been mostly supplanted by post-processing methods, which rescale abnormally high similarities between points. Early methods included combinations of local scaling [32, 57, 82], global scaling [29, 57], and centroid-scaling [27, 67, 68], but these are inefficient for large models. More scalable methods leverage a query bank to normalize abnormal retrieval similarities [4, 13, 16, 17, 63, 75]. A few are explicitly designed for cross-modal retrieval [4, 13, 75]. We evaluate their effectiveness against adversarial hubs in Section 6.

9 Conclusion and Future Work

In this paper, we revisit the well-known phenomenon of hubness, where a data point in a high-dimensional space can appear in the neighborhood of many other points that are not semantically related, and investigate how it can be exploited for adversarial purposes in multi-modal retrieval systems.

We introduce two types of adversarial hubs: (1) universal hubs that are close to, and thus retrieved by, many irrelevant user queries, and (2) concept-specific hubs that are only retrieved by queries corresponding to adversary-chosen concepts. Through empirical evaluations, we show that adversarial hubs can be crafted to appear relevant to many more queries than natural hubs. This implies that adversarial hubs could be used for spam and product promotion attacks on modern multi-modal retrieval systems that rely on pre-trained embeddings. Furthermore, we show that defenses designed to mitigate natural hubness are ineffective against concept-based adversarial hubs, motivating research on new defenses.

There are several promising directions for future exploration. On the attack side, one could apply localized perturbations-akin to adversarial patches [5]-to generate adversarial hubs, and extend their construction to modalities beyond images and audio, which are the focus of this paper. Another direction is to study adversarial hubs in the context of multi-modal RAG systems.

On the defense side, mitigating adversarial hubness is a challenge, as demonstrated in this work. Future research may focus on designing efficient detection mechanisms against adaptive attacks or investigating tradeoffs between robustness and retrieval performance in multi-modal embedding models.

Ethical Considerations

While our work investigates the vulnerability of multi-modal retrieval systems to adversarial hubs, our primary goal is to raise awareness of these threats and to inspire the development of effective defenses against adversarial hubs.

Acknowledgments

Supported in part by the NSF grant 2311521 and the Google Cyber NYC Institutional Research Program.

References

- [1] Maksym Andriushchenko, Francesco Croce, Nicolas Flammarion, and Matthias Hein. 2020. Square Attack: a query-efficient black-box adversarial attack via random search. In *European Conference on Computer Vision (ECCV)*.
- [2] Anish Athalye, Nicholas Carlini, and David Wagner. 2018. Obfuscated gradients give a false sense of security: Circumventing defenses to adversarial examples. In *International conference on machine learning*. PMLR, 274–283.
- [3] Kobus Barnard, Pinar Duygulu, David Forsyth, Nando De Freitas, David M Blei, and Michael I Jordan. 2003. Matching words and pictures. *The Journal of Machine Learning Research* 3 (2003), 1107–1135.
- [4] Simion-Vlad Bogolin, Ioana Croitoru, Hailin Jin, Yang Liu, and Samuel Albanie. 2022. Cross modal retrieval with querybank normalisation. In *Proceedings of the IEEE/CVF Conference on Computer Vision and Pattern Recognition (CVPR)*.
- [5] Tom B Brown, Dandelion Mané, Aurko Roy, Martin Abadi, and Justin Gilmer. 2017. Adversarial patch. *arXiv:1712.09665* (2017).
- [6] Nicholas Carlini, Matthew Jagielski, Christopher A Choquette-Choo, Daniel Paleka, Will Pearce, Hyrum Anderson, Andreas Terzis, Kurt Thomas, and Florian Tramèr. 2024. Poisoning web-scale training datasets is practical. In *IEEE Symposium on Security and Privacy (S&P)*. 407–425.
- [7] Nicholas Carlini, Milad Nasr, Christopher A. Choquette-Choo, Matthew Jagielski, Irena Gao, Anas Awadalla, Pang Wei Koh, Daphne Ippolito, Katherine Lee, Florian Tramèr, and Ludwig Schmidt. 2023. Are aligned neural networks adversarially aligned? *arXiv:2306.15447* (2023).
- [8] Nicholas Carlini and David Wagner. 2017. Towards evaluating the robustness of neural networks. In *IEEE symposium on security and privacy (S&P)*. 39–57.
- [9] Nicholas Carlini and David Wagner. 2018. Audio adversarial examples: Targeted attacks on speech-to-text. In *IEEE Symposium on Security and Privacy Workshops*.
- [10] Harsh Chaudhari, Giorgio Severi, John Abascal, Matthew Jagielski, Christopher A Choquette-Choo, Milad Nasr, Cristina Nita-Rotaru, and Alina Oprea. 2024. Phantom: General Trigger Attacks on Retrieval Augmented Language Generation. *arXiv:2405.20485* (2024).
- [11] Xinlei Chen, Hao Fang, Tsung-Yi Lin, Ramakrishna Vedantam, Saurabh Gupta, Piotr Dollár, and C Lawrence Zitnick. 2015. Microsoft coco captions: Data collection and evaluation server. *arXiv:1504.00325* (2015).
- [12] Mehdi Cherti, Romain Beaumont, Ross Wightman, Mitchell Wortsman, Gabriel Ilharco, Ade Gordon, Christoph Schuhmann, Ludwig Schmidt, and Jenia Jitsev. 2023. Reproducible Scaling Laws for Contrastive Language-Image Learning. In *Proceedings of the IEEE/CVF Conference on Computer Vision and Pattern Recognition (CVPR)*.
- [13] Neil Chowdhury, Franklin Wang, Sumedh Shenoy, Douwe Kiela, Sarah Schwettmann, and Tristan Thrush. 2024. Nearest Neighbor Normalization Improves Multimodal Retrieval. In *Proceedings of the 2024 Conference on Empirical Methods in Natural Language Processing (EMNLP)*.
- [14] Google Cloud. 2025. Embeddings APIs Overview. <https://cloud.google.com/vertex-ai/generative-ai/docs/embeddings>. Accessed: 2025-04-09.
- [15] Jeremy Cohen, Elan Rosenfeld, and Zico Kolter. 2019. Certified adversarial robustness via randomized smoothing. In *international conference on machine learning (ICML)*. PMLR, 1310–1320.
- [16] Alexis Conneau, Guillaume Lample, Marc’Aurelio Ranzato, Ludovic Denoyer, and Hervé Jégou. 2018. Word translation without parallel data. *International Conference on Learning Representations (ICLR)* (2018).
- [17] Georgiana Dinu, Angeliki Lazaridou, and Marco Baroni. 2014. Improving zero-shot learning by mitigating the hubness problem. *arXiv:1412.6568* (2014).
- [18] Yinpeng Dong, Huanran Chen, Jiawei Chen, Zhengwei Fang, Xiao Yang, Yichi Zhang, Yu Tian, Hang Su, and Jun Zhu. 2023. How robust is google’s bard to adversarial image attacks? *arXiv:2309.11751* (2023).
- [19] Zhihao Dou, Xin Hu, Haibo Yang, Zhuqing Liu, and Minghong Fang. 2024. Adversarial Attacks to Multi-Modal Models. *arXiv:2409.06793* (2024).
- [20] Arthur Flexer, Monika Dörfler, Jan Schlüter, and Thomas Grill. 2018. Hubness as a case of technical algorithmic bias in music recommendation. In *2018 IEEE International Conference on Data Mining Workshops (ICDMW)*.
- [21] Kuofeng Gao, Yang Bai, Jiawang Bai, Yong Yang, and Shu-Tao Xia. 2024. Adversarial Robustness for Visual Grounding of Multimodal Large Language Models. In *ICLR 2024 Workshop on Reliable and Responsible Foundation Models*.
- [22] Rohit Girdhar, Alaaeldin El-Nouby, Zhuang Liu, Mannat Singh, Kalyan Vasudev Alwala, Armand Joulin, and Ishan Misra. 2023. ImageBind: One embedding space to bind them all. In *IEEE/CVF Conference on Computer Vision and Pattern Recognition (CVPR)*.
- [23] Ian J Goodfellow, Jonathon Shlens, and Christian Szegedy. 2015. Explaining and harnessing adversarial examples. In *International Conference on Learning Representations (ICLR)*.
- [24] Sven Gowal, Krishnamurthy Dvijotham, Robert Stanforth, Rudy Bunel, Chongli Qin, Jonathan Uesato, Relja Arandjelovic, Timothy A Mann, and Pushmeet Kohli. 2018. On the effectiveness of interval bound propagation for training verifiably robust models. *arXiv 2018*. *arXiv:1810.12715* (2018).
- [25] C Guo, M Rana, M Cisse, and L Van Der Maaten. 2021. Countering adversarial images using input transformations. *arXiv 2017*. *arXiv:1711.00117* (2017).
- [26] Andrey Guzhov, Federico Raue, Jörn Hees, and Andreas Dengel. 2022. AudioCLIP: Extending CLIP to Image, Text and Audio. In *IEEE International Conference on Acoustics, Speech and Signal Processing (ICASSP)*.
- [27] Kazuo Hara, Ikumi Suzuki, Masashi Shimbo, Kei Kobayashi, Kenji Fukumizu, and Miloš Radovanović. 2015. Localized centering: Reducing hubness in large-sample data. In *Proceedings of the AAAI Conference on Artificial Intelligence (AAAI)*.
- [28] Warren He, James Wei, Xinyun Chen, Nicholas Carlini, and Dawn Song. 2017. Adversarial example defense: Ensembles of weak defenses are not strong. In *11th USENIX workshop on offensive technologies (WOOT 17)*.
- [29] Katherina Hoedt, Arthur Flexer, and Gerhard Widmer. 2022. Defending a Music Recommender Against Hubness-Based Adversarial Attacks. In *Proceedings of the 19th Sound and Music Computing Conference (SMC)*.
- [30] Hossein Hosseini, Sreeram Kannan, Baosen Zhang, and Radha Poovendran. 2017. Deceiving Google’s perspective API built for detecting toxic comments. *arXiv:1702.08138* (2017).
- [31] Matthew Jagielski, Giorgio Severi, Niklas Poussette Harger, and Alina Oprea. 2021. Subpopulation data poisoning attacks. In *Proceedings of the 2021 ACM SIGSAC Conference on Computer and Communications Security (CCS)*. 3104–3122.
- [32] Herve Jegou, Hedi Harzallah, and Cordelia Schmid. 2007. A contextual dissimilarity measure for accurate and efficient image search. In *IEEE/CVF Conference on Computer Vision and Pattern Recognition (CVPR)*.
- [33] Jiwoon Jeon, Victor Lavrenko, and Raghavan Manmatha. 2003. Automatic image annotation and retrieval using cross-media relevance models. In *Proceedings of the 26th annual international ACM SIGIR conference on Research and development in information retrieval (SIGIR)*.
- [34] Robin Jia and Percy Liang. 2017. Adversarial Examples for Evaluating Reading Comprehension Systems. In *Conference on Empirical Methods in Natural Language Processing (EMNLP)*.
- [35] Auguste Kerckhoffs. 2023. *La cryptographie militaire*. BoD—Books on Demand.
- [36] Chris Dongjoo Kim, Byeongchang Kim, Hyunmin Lee, and Gunhee Kim. 2019. AudioCaps: Generating captions for audios in the wild. In *Proceedings of the 2019 Conference of the North American Chapter of the Association for Computational Linguistics: Human Language Technologies (NAACL)*.
- [37] Minseon Kim, Jihoon Tack, and Sung Ju Hwang. 2020. Adversarial self-supervised contrastive learning. In *Annual Conference on Neural Information Processing Systems (NeurIPS)*.
- [38] Alex Krizhevsky. 2009. *Learning Multiple Layers of Features from Tiny Images*. Technical Report. University of Toronto. <https://www.cs.toronto.edu/~kriz/learning-features-2009-TR.pdf>
- [39] Hyun Kwon, Yongchul Kim, Ki-Woong Park, Hyunsoo Yoon, and Daeseon Choi. 2018. Multi-Targeted Adversarial Example in Evasion Attack on Deep Neural Network. *IEEE Access* 6 (2018), 46084–46096.
- [40] Angeliki Lazaridou, Georgiana Dinu, and Marco Baroni. 2015. Hubness and pollution: Delving into cross-space mapping for zero-shot learning. In *Proceedings of the 53rd Annual Meeting of the Association for Computational Linguistics (ACL)*.

- [41] Fangyu Liu, Rongtian Ye, Xun Wang, and Shuaipeng Li. 2020. HAL: Improved text-image matching by mitigating visual semantic hubs. In *Proceedings of the AAAI conference on artificial intelligence (AAAI)*.
- [42] Yanpei Liu, Xinyun Chen, Chang Liu, and Dawn Song. 2017. Delving into transferable adversarial examples and black-box attacks. In *International Conference on Learning Representations (ICLR)*.
- [43] Zihao Liu, Qi Liu, Tao Liu, Nuo Xu, Xue Lin, Yanzhi Wang, and Wujie Wen. 2019. Feature distillation: Dnn-oriented JPEG compression against adversarial examples. In *2019 IEEE/CVF Conference on Computer Vision and Pattern Recognition (CVPR)*.
- [44] Thomas Low, Christian Borgelt, Sebastian Stober, and Andreas Nürnberger. 2013. The hubness phenomenon: Fact or artifact? *Towards Advanced Data Analysis by Combining Soft Computing and Statistics* (2013), 267–278.
- [45] David G Lowe. 2004. Distinctive image features from scale-invariant keypoints. *International journal of computer vision* 60 (2004), 91–110.
- [46] Aleksander Madry, Aleksandar Makelov, Ludwig Schmidt, Dimitris Tsipras, and Adrian Vladu. 2018. Towards Deep Learning Models Resistant to Adversarial Attacks. In *International Conference on Learning Representations (ICLR)*.
- [47] Seyed-Mohsen Moosavi-Dezfooli, Alhussein Fawzi, Omar Fawzi, and Pascal Frossard. 2017. Universal Adversarial Perturbations. In *Proceedings of the IEEE Conference on Computer Vision and Pattern Recognition (CVPR)*.
- [48] Aaron van den Oord, Yazhe Li, and Oriol Vinyals. 2018. Representation learning with contrastive predictive coding. *arXiv:1807.03748* (2018).
- [49] OpenAI. 2023. GPT-4 Technical Report. <https://openai.com/research/gpt-4>. Accessed: 2025-04-09.
- [50] Raghuvver Peri, Sai Muralidhar Jayanthi, Srikanth Ronanki, Anshu Bhatia, Karel Mundnich, Saket Dingliwal, Nilaksh Das, Zejiang Hou, Goeric Huybrechts, Srikanth Vishnubhotla, et al. 2024. SpeechGuard: Exploring the adversarial robustness of multimodal large language models. *arXiv:2405.08317* (2024).
- [51] Pinecone. 2024. Pinecone - Vector Database for Machine Learning. <https://www.pinecone.io>. Accessed: 2024-11-12.
- [52] Xiangyu Qi, Kaixuan Huang, Ashwinee Panda, Mengdi Wang, and Prateek Mittal. 2023. Visual Adversarial Examples Jailbreak Aligned Large Language Models. In *International Conference on Machine Learning (ICML) Workshop on New Frontiers in Adversarial Machine Learning*.
- [53] Alec Radford, Jong Wook Kim, Chris Hallacy, Aditya Ramesh, Gabriel Goh, Sandhini Agarwal, Girish Sastry, Amanda Askell, Pamela Mishkin, Jack Clark, et al. 2021. Learning transferable visual models from natural language supervision. In *International conference on machine learning (ICML)*.
- [54] Milos Radovanovic, Alexandros Nanopoulos, and Mirjana Ivanovic. 2010. Hubs in space: Popular nearest neighbors in high-dimensional data. *Journal of Machine Learning Research (JMLR)* 11, 9 (2010), 2487–2531.
- [55] Gerard Salton and Christopher Buckley. 1988. Term-weighting approaches in automatic text retrieval. *Information processing & management* 24, 5 (1988), 513–523.
- [56] Amaia Salvador, Nicholas Hynes, Yusuf Aytar, Javier Marin, Ferda Ofli, Ingmar Weber, and Antonio Torralba. 2017. Learning cross-modal embeddings for cooking recipes and food images. In *Proceedings of the IEEE conference on computer vision and pattern recognition (CVPR)*.
- [57] Dominik Schmitzer, Arthur Flexer, Markus Schedl, and Gerhard Widmer. 2012. Local and global scaling reduce hubs in space. *Journal of Machine Learning Research (JMLR)* 13 (2012), 2871–2902.
- [58] Florian Schroff, Dmitry Kalenichenko, and James Philbin. 2015. FaceNet: A unified embedding for face recognition and clustering. In *Proceedings of the IEEE conference on computer vision and pattern recognition (CVPR)*.
- [59] Ali Shafahi, W Ronny Huang, Mahyar Najibi, Octavian Suciuc, Christoph Studer, Tudor Dumitras, and Tom Goldstein. 2018. Poison frogs! targeted clean-label poisoning attacks on neural networks. In *Proceedings of the 32nd International Conference on Neural Information Processing Systems (NeurIPS)*.
- [60] Avital Shafraan, Roei Schuster, and Vitaly Shmatikov. 2024. Machine Against the RAG: Jamming Retrieval-Augmented Generation with Blocker Documents. *arXiv:2406.05870* (2024).
- [61] Erfan Shayegani, Yue Dong, and Nael Abu-Ghazaleh. 2023. Plug and Pray: Exploiting off-the-shelf components of Multi-Modal Models. *arXiv:2307.14539* (2023).
- [62] Richard Shin, Dawn Song, et al. 2017. Jpeg-resistant adversarial images. In *NIPS 2017 workshop on machine learning and computer security*, Vol. 1, 8.
- [63] Samuel L Smith, David HP Turban, Steven Hamblin, and Nils Y Hammerla. 2017. Offline bilingual word vectors, orthogonal transformations and the inverted softmax. In *International Conference on Learning Representations (ICLR)*.
- [64] Spotify for Artists. 2023. Artificial Streaming. <https://artists.spotify.com/artificial-streaming>. Accessed: 2024-11-13.
- [65] Fnu Suya, Jianfeng Chi, David Evans, and Yuan Tian. 2020. Hybrid batch attacks: Finding black-box adversarial examples with limited queries. In *29th USENIX Security Symposium (USENIX Security 20)*. 1327–1344.
- [66] Fnu Suya, Saeed Mahloujifar, Anshuman Suri, David Evans, and Yuan Tian. 2021. Model-targeted poisoning attacks with provable convergence. In *International Conference on Machine Learning (ICML)*. PMLR, 10000–10010.
- [67] Ikumi Suzuki, Kazuo Hara, Masashi Shimbo, Yuji Matsumoto, and Marco Saerens. 2012. Investigating the effectiveness of Laplacian-based kernels in hub reduction. In *Proceedings of the AAAI Conference on Artificial Intelligence (AAAI)*.
- [68] Ikumi Suzuki, Kazuo Hara, Masashi Shimbo, Marco Saerens, and Kenji Fukumizu. 2013. Centering similarity measures to reduce hubs. In *Proceedings of the 2013 conference on empirical methods in natural language processing (EMNLP)*.
- [69] C Szegedy. 2014. Intriguing properties of neural networks. In *International Conference on Learning Representations (ICLR)*.
- [70] Florian Tramer and Dan Boneh. 2019. Adversarial training and robustness for multiple perturbations. *Advances in neural information processing systems* 32 (2019).
- [71] Catherine Wah, Steve Branson, Peter Welinder, Pietro Perona, and Serge Belongie. 2011. The caltech-ucsd birds-200-2011 dataset. (2011).
- [72] Bokun Wang, Yang Yang, Xing Xu, Alan Hanjalic, and Heng Tao Shen. 2017. Adversarial cross-modal retrieval. In *Proceedings of the 25th ACM international conference on Multimedia (ACM MM)*.
- [73] Kaiye Wang, Qiyue Yin, Wei Wang, Shu Wu, and Liang Wang. 2016. A comprehensive survey on cross-modal retrieval. *arXiv:1607.06215* (2016).
- [74] Tianshi Wang, Fengling Li, Lei Zhu, Jingjing Li, Zheng Zhang, and Heng Tao Shen. 2024. Cross-modal retrieval: a systematic review of methods and future directions. *Proc. IEEE* 112, 11 (2024), 1716–1754.
- [75] Yimu Wang, Xiangru Jian, and Bo Xue. 2023. Balance Act: Mitigating Hubness in Cross-Modal Retrieval with Query and Gallery Banks. In *Proceedings of the 2023 Conference on Empirical Methods in Natural Language Processing (EMNLP)*.
- [76] Eric Wong and Zico Kolter. 2018. Provable defenses against adversarial examples via the convex outer adversarial polytope. In *International conference on machine learning (ICML)*. PMLR, 5286–5295.
- [77] Chen Henry Wu, Jing Yu Koh, Ruslan Salakhutdinov, Daniel Fried, and Aditi Raghunathan. 2024. Adversarial Attacks on Multimodal Agents. *arXiv:2406.12814* (2024).
- [78] Jun Xu, Tao Mei, Ting Yao, and Yong Rui. 2016. MSR-VTT: A large video description dataset for bridging video and language. In *Proceedings of the IEEE conference on computer vision and pattern recognition (CVPR)*. 5288–5296.
- [79] Weilin Xu, David Evans, and Yanjun Qi. 2017. Feature squeezing: Detecting adversarial examples in deep neural networks. *arXiv:1704.01155* (2017).
- [80] Jiaqi Xue, Mengxin Zheng, Yebowen Hu, Fei Liu, Xun Chen, and Qian Lou. 2024. BadRAG: Identifying Vulnerabilities in Retrieval Augmented Generation of Large Language Models. *arXiv:2406.00083* (2024).
- [81] Qiyue Yin, Jieming Lou, Xianyuan Zhan, Qizhang Li, Wangmeng Zuo, Yang Liu, and Jingjing Liu. 2022. Adversarial contrastive learning via asymmetric InfoNCE. In *European Conference on Computer Vision (ECCV)*.
- [82] Lihi Zelnik-Manor and Pietro Perona. 2004. Self-tuning spectral clustering. In *Proceedings of the 17th International Conference on Neural Information Processing Systems (NeurIPS)*.
- [83] Collin Zhang, Tingwei Zhang, and Vitaly Shmatikov. 2024. Controlled Generation of Natural Adversarial Documents for Stealthy Retrieval Poisoning. *arXiv:2410.02163* (2024).
- [84] Hongyang Zhang, Yaodong Yu, Jiantao Jiao, Eric Xing, Laurent El Ghaoui, and Michael Jordan. 2019. Theoretically principled trade-off between robustness and accuracy. In *International conference on machine learning (ICML)*. PMLR, 7472–7482.
- [85] Tingwei Zhang, Rishi Jha, Eugene Bagdasaryan, and Vitaly Shmatikov. 2024. Adversarial illusions in multi-modal embeddings. In *33rd USENIX Security Symposium (USENIX Security)*.
- [86] Tingwei Zhang, Collin Zhang, John X Morris, Eugene Bagdasarian, and Vitaly Shmatikov. 2024. Soft Prompts Go Hard: Steering Visual Language Models with Hidden Meta-Instructions. *arXiv:2407.08970* (2024).
- [87] Yunqing Zhao, Tianyu Pang, Chao Du, Xiao Yang, Chongxuan Li, Ngai-Man Cheung, and Min Lin. 2023. On evaluating adversarial robustness of large vision-language models. In *Annual Conference on Neural Information Processing Systems (NeurIPS)*.
- [88] Zexuan Zhong, Ziqing Huang, Alexander Wettig, and Danqi Chen. 2023. Poisoning retrieval corpora by injecting adversarial passages. In *Proceedings of the 2023 Conference on Empirical Methods in Natural Language Processing (EMNLP)*. 13764–13775.
- [89] Ziqi Zhou, Shengshan Hu, Ruizhi Zhao, Qian Wang, Leo Yu Zhang, Junhui Hou, and Hai Jin. 2023. Downstream-agnostic adversarial examples. In *IEEE International Conference on Computer Vision (ICCV)*.
- [90] Andy Zou, Zifan Wang, J Zico Kolter, and Matt Fredrikson. 2023. Universal and transferable adversarial attacks on aligned language models. *arXiv:2307.15043* (2023).
- [91] Wei Zou, Rungpeng Geng, Binghui Wang, and Jinyuan Jia. 2024. PoisonedRAG: Knowledge corruption attacks to retrieval-augmented generation of large language models. *arXiv:2402.07867* (2024).